Molecular & Biochemical Parasitology 219 (2018) 33–41

Contents lists available at ScienceDirect

Molecular & Biochemical Parasitology

journal homepage: www.elsevier.com/locate/molbiopara

Research Paper

TbVps15 is required for vesicular transport and cytokinesis in *Trypanosoma brucei*

Alejandra C. Schoijet[a,b], Kildare Miranda[c,d], Tamara Sternlieb[a], Nadia M. Barrera[a], Wendell Girard-Dias[c,e], Wanderley de Souza[c,d], Guillermo D. Alonso[a,b,*]

[a] *Instituto de Investigaciones en Ingeniería Genética y Biología Molecular "Dr. Héctor N. Torres" (INGEBI-CONICET), Buenos Aires, Argentina*
[b] *Universidad de Buenos Aires, Facultad de Ciencias Exactas y Naturales, Departamento de Fisiología, Biología Molecular y Celular, Buenos Aires, Argentina*
[c] *Laboratorio de Ultraestrutura Celular Hertha Meyer, Instituto de Biofísica Carlos Chagas Filho and Centro Nacional de Biologia Estrutural e Bioimagem (CENABIO), Universidade Federal do Rio de Janeiro, Rio de Janeiro, Brazil*
[d] *Instituto Nacional de Biologia Estrutural e Bioimagem, Universidade Federal do Rio de Janeiro, Rio de Janeiro, Brazil*
[e] *Plataforma de Microscopia Eletrônica Rudolf Barth IOC, Fiocruz, Rio de Janeiro, Brazil*

ARTICLE INFO

Keywords:
Trypanosoma brucei
TbVps15 protein kinase
Cell cycle
Endocytosis

ABSTRACT

The class III phosphatidylinositol 3-kinase (PI3K) Vps34 is an important regulator of key cellular functions, including cell growth, survival, intracellular trafficking, autophagy and nutrient sensing. In yeast, Vps34 is associated with the putative serine/threonine protein kinase Vps15, however, its role in signaling has not been deeply evaluated. Here, we have identified the Vps15 orthologue in *Trypanosoma brucei*, named TbVps15. Knockdown of TbVps15 expression by interference RNA resulted in inhibition of cell growth and blockage of cytokinesis. Scanning electron microcopy revealed a variety of morphological abnormalities, with enlarged parasites and dividing cells that often exhibited a detached flagellum. Transmission electron microscopy analysis of TbVps15 RNAi cells showed an increase in intracellular vacuoles of the endomembrane system and some cells displayed an enlargement of the flagellar pocket, a common feature of cells defective in endocytosis. Moreover, uptake of dextran, transferrin and Concanavalin A was impaired. Finally, TbVps15 downregulation affected the PI3K activity, supporting the hypothesis that TbVps15 and TbVps34 form a complex as occurs in other organisms. In summary, we propose that TbVps15 has a role in the maintenance of cytokinesis, endocytosis and intracellular trafficking in *T. brucei*.

1. Introduction

The phosphatidylinositol (PtdIns) 3-kinase (PI3K) Vps34, that phosphorylates the D3 hydroxyl of phosphatidylinositol to form phosphatidylinositol 3-phosphate (PI3P), is a crucial enzyme conserved in all eukaryotes, and plays important roles in endocytic trafficking, autophagy, phagocytosis, cytokinesis and nutrient sensing [1–3]. Vps34 exerts its function by associating into a protein complex with a serine/threonine kinase named Vps15. In yeast, the complex I: Vps34, Vps15, Vps30 (known as Beclin 1 in mammals, also called Atg6), Atg14 and Atg38 is implicated in autophagy, whereas complex II: Vps34, Vps15, Vps30 and Vps38 (known as UVRAG in mammals) is involved in membrane trafficking [4]. In mammals, Atg14 and UVRAG bind Beclin 1 in a mutually exclusive manner and distinguish between two functionally different phosphatidylinositol 3-kinase (PI3K) complexes (Atg14 complex and UVRAG complexes), which are involved in different steps of the autophagic process and also endocytic trafficking. Atg14 associates with the core Beclin 1-Vps34-Vps15 complex and targets this complex to the endoplasmatic reticulum to exert its function in the biosynthesis of autophagosomes. On the other hand, UVRAG participates promoting autophagosome maturation, endocytosis and cytokinesis (activating UVRAG complex) or inhibiting the maturation of autophagosomes (inhibitory UVRAG complex) according to which adapter proteins are attached to [5]. Of these PI3K complex proteins, Vps15 remains an understudied kinase, and its function has not been rigorously investigated in multicellular organisms *in vivo*. Most of the focus on the role of these complexes has been on nutrient deprivation-autophagy.

Previously, we have reported the cloning and characterization of both TcVps34 and TcVps15 in *Trypanosoma cruzi* and demonstrated that in this parasite these proteins function as a complex [6,7]. In addition, we demonstrated that TcVps34 plays a prominent role in vital processes

* Corresponding author at: Laboratorio de señalización y mecanismos adaptativos en Tripanosomátidos, Instituto de Investigaciones en Ingeniería Genética y Biología Molecular "Dr. Héctor N. Torres" (INGEBI-CONICET), Vuelta de Obligado 2490 (C1428ADN), Buenos Aires, Argentina.
E-mail addresses: galonso@dna.uba.ar, buiyimail@gmail.com (G.D. Alonso).

https://doi.org/10.1016/j.molbiopara.2017.11.004
Received 9 May 2017; Received in revised form 10 November 2017; Accepted 11 November 2017
Available online 16 November 2017
0166-6851/

for *T. cruzi* survival such as osmoregulation, acidification, endocytosis and vesicular trafficking, and that both TcVps34 and TcVps15 are involved in autophagy in this parasite. Moreover, TcVps34 subcellular localization was affected and its lipid kinase activity was reduced in parasites expressing a catalytic domain mutated version of TcVps15, proposing a role of TcVps15 as a key regulator of TcVps34. This complex is in addition related to the cAMP pathway through the TcrPDEC2 phosphodiesterase, also characterized in our laboratory, which it is also involved in osmoregulation in *T. cruzi*, and possesses a FYVE domain, which is known to serve as a lipid signal for membrane recruitment of proteins [8,9]. In *Trypanosoma brucei*, the orthologue protein TbVps34 has also been characterized, and RNAi experiments demonstrated a role in segregation of the Golgi apparatus at cytokinesis [10].

Trypanosoma brucei, an extracellular protozoan parasite, is the causative agent of African sleeping sickness in humans. The parasite exists in two distinct life forms, the mammalian bloodstream form and the insect procyclic form. *T. brucei* has a highly polarized exocytic and endocytic system, which is located between the nucleus and a specialized section of the plasma membrane called the flagellar pocket. Endocytosis at the flagellar pocket is important in both forms for uptake of nutrients and for host-parasite interactions, holding a role in immune evasion. In this sense, it is important to point out that trafficking, endocytosis, and Golgi maintenance are all PtdIns-mediated events in other eukaryotes [11].

In the present study, we have functionally characterized, in *T. brucei*, the serine/threonine kinase TbVps15 by using RNAi experiments. We show that TbVps15 is essential for normal growth and morphology in procyclic parasites. In addition, our analysis revealed that TbVps15 is required for endocytosis, protein trafficking and cytokinesis.

2. Materials and methods

2.1. Chemicals and reagents

All radiochemicals used in this work were purchased from Perkin Elmer Life Sciences, and restriction endonucleases were from New England Biolabs, Beverly, MA. Bactotryptose, yeast nitrogen base, and liver infusion were from Difco. All other reagents were purchased from Sigma.

2.2. Trypanosome cell culture and transfection

Procyclic culture form 29-13 cells (a generous gift of George Cross, Rockefeller University), which stably express T7 polymerase and a tetracycline repressor, were used for creating RNAi cell lines [12]. 29-13 parental line cultures were grown in SDM-79 supplemented with 10% FBS in the presence of 25 μg/ml G418 and 25 μg/ml hygromycin. Cells were counted daily using a Neubauer hemocytometer, and cultures were diluted to 5×10^5 cells/ml when the density approached 10^7 cells/ml.

2.3. Generation and induction of TbVps15 RNAi

The gene sequence corresponding to the *Saccharomyces cerevisiae* Vps15 (ID 852394) was used to screen *T. brucei* sequences in the GeneDB database using the WU-Blast2 algorithm. As result of this search, a high-scored target was detected: Tb927.11.9190. Appropriate oligonucleotide pairs: TbVps15-Fw-SpeI 5′ACTAGTAAGCGGCTTTTAC TTCGTCAG3′ and TbVps15-Rv-HindIII

5′AAGCTTTTGCACGACTTTATTGCTCG3′ were designed for the production of RNAi construct, using the RNAit-target selection script on the *T. brucei* functional genomics website (TrypanoFAN) [13]. RNAi target was amplified using ~400 ng from *T. brucei* Lister 427 genomic DNA, 100 ng of each primer, 2.5 mM $MgCl_2$, 0.2 mM dNTPs and 2 units of Invitrogen™ Platinum™ DNA Polymerase. Amplification product was first cloned into pGEM-T Easy vector (Promega, Madison, WI, USA) and then subcloned into the p2T7Ti-177 vector [14]. Cells of the 29-13 strain were transfected by electroporation as follows. Briefly, 1×10^8 cells were harvested, washed twice with cytomix buffer (120 mM KCl; 0.15 mM $CaCl_2$; 10 mM K_2HPO_4; 25 mM Hepes; 2 mM EGTA; 5 mM $MgCl_2$; 2 mM ATP; 5 mM glutathione; pH adjusted to 7.6 with KOH) and suspended in 0.45 ml of cytomix buffer containing 10 μg of the NotI linearized construct. Electroporation was carried out using a Bio-Rad electroporator with peak discharge at 1.6 kV and 25 μF of capacitance. The transfected cells were immediately transferred into 10 ml of SDM-79 supplemented with G418 and hygromycin. The transfectants were selected under 2.5 μg/ml phleomycin with individual cells cloned by limiting dilutions, generating independent TbVps15 RNAi cell lines. The stable transfectants thus obtained were then induced with 1 μg/ml tetracycline to switch on the T7 promoter, to initiate the TbVps15 RNAi. Cells in the presence (+Tet) or absence (−Tet) of tetracycline were counted daily and cumulative growth curves for each clone were plotted on a logarithmic scale.

2.4. Sequence analysis

The search in *T. brucei* genome database (http://www.genedb.org) was performed with Wu-Blast2. Sequence identity and similarity were analyzed with the EMBOSS Needle Pairwise Sequence Alignment tool with default parameters settings (Matrix: BLOSUM62, gap open penalty: 10 and gap extend penalty: 0.5). Protein domains were determined using SMART (URL http://smart.embl-heidelberg.de/), and PROSITE (URL http://us.expasy.org/prosite/) software.

2.5. Northern blot analysis

Total RNA was obtained from *T. brucei* using TRIzol reagent (Invitrogen, Carlsbad, California, USA) according to the manufacturer's instructions and Northern blotted as previously described by Alonso et al. [15]. Probe for TbVps15 was 498 bp fragment used for RNAi. The probe was labelled with [α-^{32}P]-dCTP using the Prime-a-Gene kit (Promega, Madison, WI, USA) following the manufacturer's instructions.

2.6. Hydroxyurea-induced synchronization of T. brucei cell cycle

Synchronization of the procyclic forms of *T. brucei* in S phase using hydroxyurea (HU) was essentially as described in Chowdhury et al. [16]. Briefly, 10 ml culture (2.5×10^6 cells/ml) was incubated in medium containing 0.2 mM HU for 12 h. Then the HU was removed by centrifugation (1200*g*, 10 min) and the cells were washed twice with medium at room temperature. After washout of HU, cells continued to be cultured for 12 h. To assess synchrony, we fixed cells every 2 h, stained them with propidium iodide, and conducted flow cytometry. Cell samples for flow cytometry analysis were prepared as follows. Briefly, 1×10^6 cells harvested at different times by centrifugation at 600*g* for 10 min were washed twice with cold PBS plus 2 mM EDTA. The cell pellets were resuspended in 200 μl PBS plus 2 mM EDTA and fixed by adding 1.5 ml of 70% ethanol in PBS dropwise while vortexing. Samples were stored at 4 °C overnight. The fixed cells were washed with PBS and then suspended in 1 ml of PBS containing DNase-free RNase A (10 μg/ml) and propidium iodide (PI) (20 μg/ml). The mixture was incubated at 37 °C for 30 min and then analyzed using a FACS flow cytometer (FACS Aria, Becton Dickinson). Percentages of cells at different phases of the cell cycle were evaluated by Cyflogic software.

2.7. Analysis of the arrangement of nuclei and kinetoplasts

T. brucei cells were harvested, washed three times with PBS, and fixed on slides with 4% formaldehyde at 4 °C for 30 min. Slides were washed with PBS in the presence of 1 μg/ml of DAPI. Subsequently,

cells were examined with an Olympus IX-71 inverted fluorescence microscope. The numbers of nuclei and kinetoplasts in individual cells were tabulated in populations of more than 200 cells in each sample.

2.8. Endocytosis assays

RNAi was induced by incubation for three days with 1 μg/ml tetracycline. To analyze co-localization with the lysosome, we use red or green LysoTracker (10 μM) as appropriate, a fluorescent acidotropic reagent that traces acidic organelles in cells and has previously been used to stain the parasite lysosome [17]. Cells were harvested and washed once in serum-free SDM-79 medium containing 1% BSA. After that, cells were incubated in serum-free SDM-79/BSA at 28 °C for 30 min and then LysoTracker was added and incubated for 1 h. To follow endocytosis, FITC-conjugated Concanavalin A (FITC-ConA) (Molecular Probes) (100 μg/ml), Alexa Fluor 546 dextran 10000 (Molecular Probes) (5 mg/ml) or FITC-transferrin (Molecular Probes) (100 μg/ml) were individually added, and cells were incubated for another 30 min. Uptake was stopped by the addition of 1 ml of ice-cold SDM-79 medium, and the cells were washed once at 4 °C before fixing for 30 min at 4 °C in 4% formaldehyde. The cells were adhered to slides, mounted, and examined immediately. The images were taken under non-saturating conditions using identical exposure times.

Quantification was performed by flow cytometry (FACS Aria, Becton Dickinson). The values are presented as the mean fluorescence intensity (MFI) of the induced or non-induced parasites minus the MFI corresponding to parasites without tracer.

2.9. Scanning electron microscopy

About 1×10^8 procyclic forms were harvested and washed twice with PBS. The parasites were fixed with freshly prepared 2.5% glutaraldehyde, 4% formaldehyde, 0.1 M sodium cacodylate buffer, pH 7.3, for 1 h at 4 °C, adhered to poly-L-lysine-coated coverslips, dehydrated in ethanol series, critical point dried, and coated with gold in a Balzers gold sputtering system. Cells were observed in a JEOL JSM 6340F field emission scanning electron microscope operating at 5 kV.

2.10. Live cell imaging

For live cell video-microscopy, parasites were mounted in SDM-79 medium and videos of 10 s of duration were immediately captured using an Olympus BX41 fluorescence microscope. Cells were observed at 100X with differential interference contrast (DIC).

2.11. Transmission electron microscopy

Cells were harvested and washed twice with PBS. The parasites were fixed with a glutaraldehyde solution 2.5% in phosphate buffer 0.1 M pH 7.4 during 4 hs, at 4 °C, washed twice and post-fixed with 1% osmium tetroxide in the same buffer for 60 min at 4 °C. Cells were rinsed twice with double distilled water and the material was dehydrated and then embedded in epoxy resin, sectioned, and stained using standard methods for transmission electron microscopy. Images were obtained on a Zeiss 900 transmission electron microscope.

2.12. Morphometry

Volumetric density of the vesicular content was assessed in thin sections. Randomly selected cell profiles were observed and imaged in a JEOL1200 EX transmission electron microscope equipped with a Megaview G2 side-mount camera and an iTEM image analysis system. Morphometry was carried out on sections of parasites according to principle of Delesse, where a volume fraction in 3D is determined from area fraction on sections. The volume fraction (volumetric density) of the organelles is basically extrapolated from the area fraction found in thin sections. This has been routinely applied to a number of cells, including protozoan parasites [18,19]. Profiles of 30 cells in each condition (uninduced and induced) were imaged and measured, as well as their vacuoles (including acidocalcisomes), when present. Results are expressed as percentage of the cell volume occupied by vacuoles (volumetric density). Statistical significance was determined by Student's *t*-test ($P \leq 0.05$).

2.13. Protein and lipid kinase activity assays

Protein kinase activity was determined as previously measured for the hVps15 [20]. Uninduced (−Tet) and induced (+Tet) parasites at day three were used to prepare the protein extracts. Briefly, 25 μg of total *T. brucei* protein extracts were incubated in 35 μl with 15 μl of a phosphorylation mixture containing 2.5 μCi of [γ-^{32}P]ATP, 10 μM ATP, 25 mM Tris-HCl pH 8.0, 20 mM $MnCl_2$, 1 mM DTT, 500 μM NaF, 400 μM Na_3VO_4 and 0.5 mg ml^{-1} of the histone H2As (Histone from calf thymus, Sigma) as substrate. After 30 min of incubation at 30 °C, the kinase reaction was stopped by spotting 40 μl of the reaction onto 2 × 2 cm squares of phosphocellulose P-81 paper. [γ-^{32}P]ATP was separated from the labeled substrate by washing the P-81 filter papers tree times for 5 min with 75 mM H_3PO_4. The paper squares were dried, and the radioactivity incorporated was determined in a liquid scintillation counter.

PI3K activity assays using *T. brucei* cell extracts were carried out as described before [6]. Briefly, 50 μg of total protein was assayed in 75 μl reactions containing 20 mM Tris-HCl, pH 7.4, 4 mM $MgCl_2$, 100 mM NaCl, 2 mg ml^{-1} sonicated phosphatidylinositol, 40 μM ATP, and 25 μCi/ml [γ-^{32}P]ATP. The mixtures were incubated at 30 °C for 15 min, and reactions were terminated by the addition of 150 μl of 1 M HCl. Lipids were extracted first with $CHCl_3$/CH_3OH (1:1) plus 10 mM EDTA, and the resulting organic phase was then extracted with CH_3OH/HCl (100:1) plus 10 mM EDTA. The obtained organic phase was dried with nitrogen gas, resuspended in $CHCl_3$/CH_3OH (1:1), and radiolabeled phosphoinositides were measured in a liquid scintillation counter.

3. Results

3.1. Identification of T. brucei TbVps15

A systematic search for a potential *Vps15* gene homolog in *T. brucei* was performed using *Saccharomyces cerevisiae* gene as query. A single homologous gene for this kinase was found in *T. brucei* Lister strain 427 genome, chromosome 11, under the gene ID Tb927.11.9190. The ORF corresponding to this putative *T. brucei* kinase-like homolog was designated as TbVps15. This predicted TbVps15 kinase is encoded by a 4113-bp ORF and consists of 1370 amino acids with a predicted molecular mass of 150.628 kDa and a calculated isoelectric point of 7.64. The predicted primary sequence of TbVps15 protein shared 49.4% of identity and 63.4% of similarity with *T. cruzi* TcVps15 (XP_819025.1), 25.8% of identity and 37.4% of similarity with the *Leishmania major* orthologue, 20.1% of identity and 33.9% of similarity with *Sacharomyces cerevisiae* ScVps15p (CBK39172) [21] and 20.7% of identity and 34.8% of similarity with the human VPS15 homologue p150 (NP_055417.1) [20].

Through a more detailed analysis, we found that TbVps15 shows the same domain distribution than the serine/threonine kinase previously characterized by our group TcVps15 [7], with an immediate N-terminal potential attachment site for myristic acid (residues 1–6), the catalytic domain (residues 52–380), shared by the serine/threonine family of protein kinases and three C-terminal WD repeats (residues 983–1021, 1,2271,268 and 1325–1367). The sequence also retains the lysine residue K220, which is well-conserved among all known serine/threonine protein kinases. In addition, we demonstrated that this residue is key for TcVps15 enzymatic activity and at the same time it is essential for

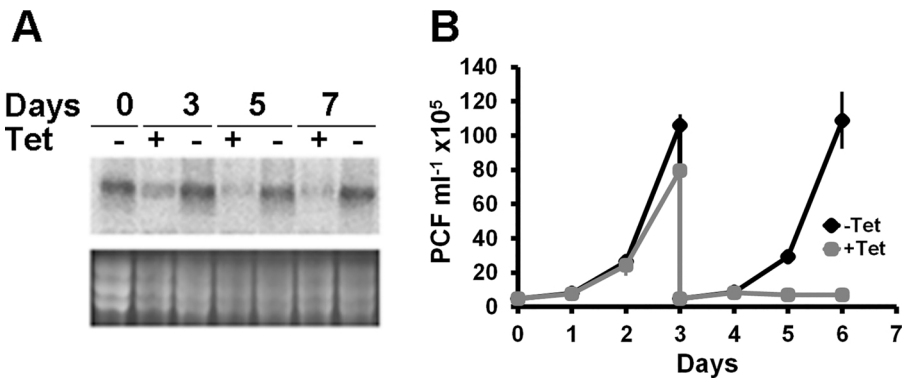

Fig. 1. TbVps15 is required for normal growth. **A**. Loss of TbVps15 RNA in cells induced for RNAi. RNA was extracted from cells incubated in the presence or absence of 1 μg/ml tetracycline for seven days and analyzed by Northern blot. rRNA was used as loading control. **B**. TbVps15 RNAi inhibits cell growth. Procyclic 29-13 cells transfected with p2T7Ti-177-TbVps15 were incubated with or without 1 μg/ml tetracycline to induce RNAi, and growth was monitored daily by cell counting with Neubauer chamber. Each point represents the mean of triplicate values.

its physiological role in *T. cruzi* [7].

3.2. TbVps15 is essential for the growth of procyclic forms of T. brucei

In order to investigate possible functional roles of TbVps15 in procyclic forms of *T. brucei*, a stable tetracycline-inducible RNAi procyclic cell line was generated, using a portion of the gene that has no significant sequence identity with other genomic sequences of *T. brucei*, subcloned into the p2T7Ti-177 vector. The effect of RNAi on TbVps15 gene expression was examined by Northern blot. After three days of tetracycline induction, transcript levels were visibly reduced and at day five then were undetectable, compared to those in the uninduced cells (Fig. 1A). To investigate the effect on cell growth of TbVps15, TbVps15-deficient parasites were counted daily during a 6- day incubation period (Fig. 1B). Uninduced cultures were used as control. A cell growth decrease was observed at the beginning of the third day after tetracycline induction of TbVps15-RNAi. Afterward, on day four, the parasites do not recover their growth by diluting them in fresh medium and by day five, there is 76% of cell death. Therefore, from here on we choose to perform all the experiments on day three after induction with tetracycline, due to at that moment we already observe a considerable decrease in the number of parasites, but without as much mortality as at days four and five. The significant inhibition of cell growth suggested that TbVps15 could play an essential role in the procyclic form of *T. brucei.*

3.3. Depletion of TbVps15 results in severe morphological defects and alteration of cell cycle

To investigate the effect of TbVps15 depletion on cell cycle progression, the kinetoplast and nuclear contents of uninduced and induced cells were analyzed in DAPI-stained cells. Fluorescence microscopy analysis of induced cultures showed the presence of an abnormal phenotype, consisting of enlarged parasites. Examination of DAPI-stained slides revealed an increase in cells with two nuclei and two kinetoplasts 72 h after induction (Fig. 2A). These observations were corroborated by quantification of the number of nuclei and kinetoplasts at days three and four (Fig. 2B). After the fourth day, the induced parasites do not recover their growth rate and a high mortality percentage is observed. The morphologically abnormal cells also exhibit defects in motility. Instead of swimming through the medium, they remain in one place. Video-microscopy revealed that the flagella of these cells were still beating, but it was wrongly positioned, in some cells detached, and its movement was not dragging cells in any direction. (Supplemental data S1–S5). In addition, scanning electron microscopy was employed to examine the surface structure of the RNAi induced cells. Induced cells revealed an abnormal morphology consisting of enlarged body cells and parasites apparently incapable of complete cell division.

Some of the induced cells also showed a detached flagellum (Fig. 2C). To further determine the defects in the progression of the cell cycle, TbVps15 cultures were induced for three days, then were synchronized with respect to DNA synthesis using hydroxyurea (HU) and progression through the cell cycle upon release of HU was evaluated by propidium iodide (PI) staining and flow cytometry analysis. In normal conditions without tetracycline, during the first 4 h, the peak traverses through S and G2, the G1 peak gradually reappears (4 h and 6 h), indicating the start of the next cycle. At 8 and 10 h, the cells again traverse through S phase, and by 12 h they begin accumulating in G2 phase for the second time. In these later stages, the peak broadens, indicating gradual loss of synchrony (Fig. 2D, left panel) [16]. On the other hand, cells induced with tetracycline had an increase in G2/M population and a corresponding decrease in G1 cells without much change in S-phase cells, indicating a delay in the cellular division (Fig. 2D, right panel). This effect is particularly visible at four hours (Vps15-depleted cells exhibited 61% in G2/M versus 50% in control cells and 12% in G1 versus 20% in control cells) and at six hours (Vps15-depleted cells showed 36% in G2/M versus 25% in control cells and 38% in G1 versus 50% respectively). It is also important to point out that induced parasites showed emergence of cells with more than 2N2K, indicating that the cells failed to divide.

Transmission electron microscopy analysis of TbVps15 RNAi cells showed an increase in intracellular vacuoles (Fig. 3A–D). Vacuoles of the endomembrane system, acidocalcisomes were bundle to the same group, since acidocalcisomes are not easily distinguished from empty vacuoles in profiles of cells submitted to chemical fixation and regular embedding for TEM analysis. Uninduced cells showed a characteristic distribution of intracellular vacuoles, occupying 1.89% of the cell volume, whereas in TbVps15 RNAi induced cells vacuoles accounted for 4.87% of the cell volume (Fig. 3E). In addition, some of the induced cells showed an enlargement of the flagellar pocket, a common feature of cells defective in endocytosis, known as “big eye” (Fig. 3F–H).

3.4. PI3K activity is diminished in TbVps15 cells

Since Vps15 forms a complex with Vps34 in some organisms, we evaluated whether suppression of TbVps15 affects overall kinase activity and PI3K activity in particular. As Fig. 4A shows, protein kinase activity in extracts from RNAi-induced TbVps15 parasites was significantly reduced when compared with extracts from uninduced cells (8.205 ± 0.512 pmol/min/mg and 11.497 ± 0.674 pmol/min/mg respectively), leading to a 28.636% decrease in kinase activity. In addition, lipid kinase activity was reduced in induced TbVps15 parasites comparing to uninduced cells (5.928 ± 0.133 pmol/min/mg and 10.925 ± 0.317 pmol/min/mg respectively), leading to a 45.736% decrease in lipid kinase activity (Fig. 4B). These results demonstrate that silencing of TbVps15 affects PI3K activity, suggesting that in *T. brucei* both proteins could also be part of a complex as occurs in other organisms.

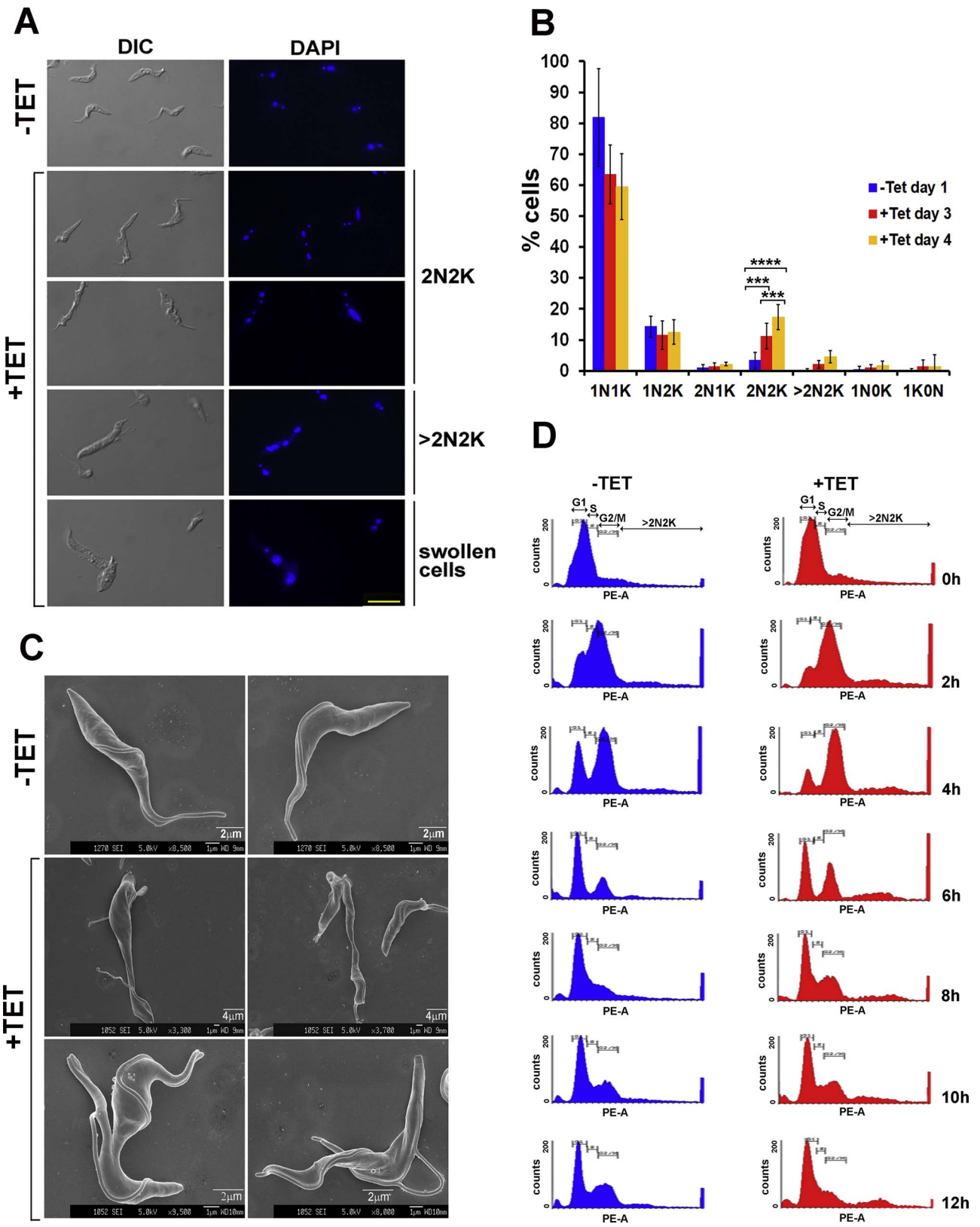

Fig. 2. TbVps15 RNAi induces a variety of morphological abnormalities and affects cell cycle. **A**. Samples of induced and uninduced parasites were taken at day three, cells were stained with DAPI and analyzed by microscopy for numbers and configurations of nucleus (N) and kinetoplast (K). Scale bar: 10 μm. **B**. Analysis of the numbers of nuclei and kinetoplasts as determined by DAPI staining of uninduced and induced parasites at days three and four. Data is presented as percentages of cells from a total number of 200 cells from three independent induction experiments. Error bars represent the standard deviation (SEM). One way Anova, Tukey's multiple comparisons test, $p < 0.0001$, **** asterisk; $p < 0.001$, *** asterisk. **C**. Scanning electron microscopic analysis of TbVps15 -depleted *T. brucei*. Scanning electron micrographs of cells depleted of TbVps15 by 3-day RNAi induction, showing enlarged parasites and parasites with detached flagella. **D**. Hydroxyurea synchronization of procyclic *T. brucei* at day three of RNAi induction. Cells were treated with 0.2 mM HU for 12 h (0 h–12 h), stained with propidium iodide, and analyzed by flow cytometry. The percentage of G1, S, and G2/M-phase cells was calculated by using the software program Cyflogic.

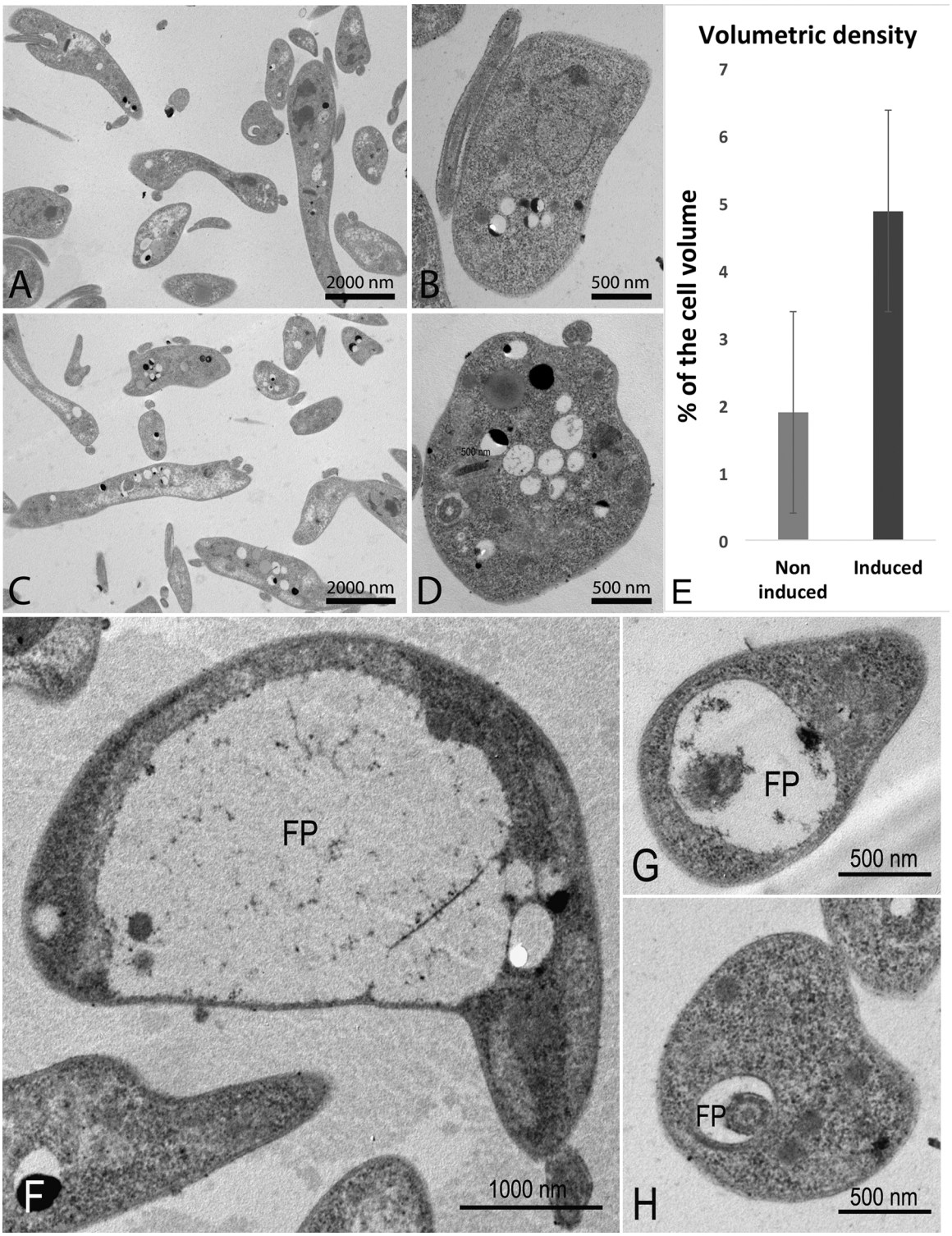

Fig. 3. TbVps15 RNAi cells showed an increase in the volume occupied by intracellular vacuoles. **A-B**. Uninduced cells, showing a characteristic distribution of intracellular vacuoles. **C-D**. Induced cells at day three showing an apparent increase in the number of intracellular vacuoles. **E**- Morphometric analysis showing an increase in the volume occupied by intracellular vacuoles in TbVps15 RNAi induced cells. P value < 0,05 on Student's *t*-test (P = 0,00185). **F-G**. Enlarged flagellar pocket in TbVps15 induced cells. **H**. Control of uninduced cells.

3.5. TbVps15 RNAi interferes with endocytosis and intracellular transport

Previously we have reported in *T. cruzi*, that TcVps15 is part of a complex together with the phosphatidylinositol 3-kinase (PI3K) TcVps34 [7]. In addition, we have determined that parasites that overexpress TcVps34 have defects in endocytosis and vesicular transport [6]. Similar effects were also observed with the orthologue protein TbVps34 in *T. brucei* [10]. Furthermore, the depletion of the PtdIns 4-kinase β (TbPIK4III-β) was found to cause defects in the Golgi and in the correct location of markers in the lysosome [22]. To determine whether TbVps15 is involved in the endocytic pathway, uptake of FITC-transferrin, FITC-Concanavalin A and Alexa Fluor 546 dextran was examined by fluorescent microscopy, using LysoTracker as a lysosome marker. In uninduced cells, the three tracers appears as a single bright

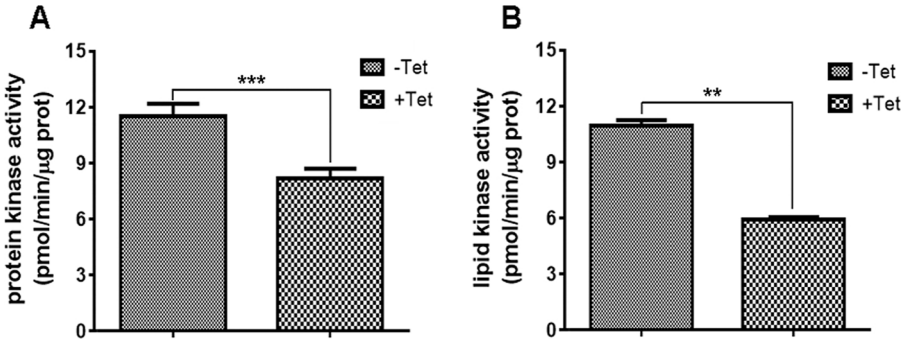

Fig. 4. Protein and lipid kinase activity in TbVps15 RNAi parasites. **A**. Protein kinase activity assays were performed as described under Material and Methods using H2As as substrate and 25 µg of total protein of uninduced (−Tet) or induced (+Tet) at day three TbVps15 parasite extracts. There was a statistically significant (*t*-test, p 0.0001, asterisk) protein kinase activity decrease in silenced TbVps15 cells. Error bars represent the standard error of the mean (SEM) of three independent experiments. **B**. Reduced lipid kinase activity in TbVps15 parasites. PI3K activity assays were performed as described under Material and Methods using 50 µg of uninduced or induced at day three TbVps15 parasite extracts. There was a statistically significant (*t*-test, p 0.014, asterisk) decrease in induced TbVps15 kinase activity.

point at the lysosome, co-localizing with the LysoTracker; however, accumulation of all the tracers was partially blocked in TbVps15 RNAi cells (Fig. 5A–C). Afterword, we used flow cytometry analysis to quantitate accumulation of transferrin, ConA and dextran in large numbers of cells (Fig. 5D–F). The incorporation of tracers, quantified as mean internal fluorescence (MFI) was 3.780 ± 0.784 times less for transferrin, 3.111 ± 0.135 times less for ConA and 2.074 ± 0.360 times less for dextran in induced parasites compared to uninduced parasites. Our data indicated a generally diminished endocytosis level of TbVps15 RNAi induced parasites as compared to the parental, uninduced ones, confirming a role for TbVps15 in this process.

4. Discussion

Previous analyses have shown that the class III PI 3-kinase Vps34 plays key roles in vesicular trafficking, endocytosis and autophagy. In addition, Vps34 forms a complex with the serine/threonine kinase adaptor protein Vps15, which also interacts with other membrane proteins, such as the Rab5 GTPase to coordinate Vps34 activity [23]. However, despite its discovery over 15 years ago, Vps15 role in Vps34 signaling has been somewhat mysterious. Previously, we have functionally characterized both Vps34 and Vps15 in *Trypanosoma cruzi*, the causative agent of Chagas disease, and demonstrated that they have a role in autophagy in this parasite [6,7]. In the present study, we showed that TbVps15 is an essential protein in the procyclic form of *Trypanosoma brucei*, as its depletion by RNAi causes severe growth and morphological defects. After day three of RNAi induction, there is a loss of transcripts, evidenced by Northern blot, and begins the appearance of abnormally shaped cells. Examination of DAPI-stained slides revealed a progressive increase in cells with two nuclei and two kinetoplastids. Moreover, by using synchronized TbVps15-RNAi cells, we showed that TbVps15 depletion has an effect on cell cycle with accumulation in the G2/M phase, indicating defects in cytokinesis. Similar results have been observed with the depletion of the PI3K TbVps34 and PI4K-IIIβ in *T. brucei* [22,24], suggesting a potential role of phosphoinositides in cellular division. Furthermore, scanning electron microscopy of induced cells displayed enlarged parasites and cells with detached flagellum, supporting an impairment on cellular division. This is consistent with the effects on cytokinesis and the observation of abnormal phenotypes in TbVps15 RNAi cultures, since the flagellum is required for the correct completion of cell division. The phenotype of elongated parasites also resembles the “nozzle” phenotype previously described by the Matthews group [25]. They observed that the overexpression of the zinc finger protein TbZFP2 produced an elongation at the posterior end of the cell, with a delay of the cell cycle at G2/M stage. However, it is not certain that the protein Matthews et al. investigated participates in the same pathways as the Vps34/Vps15 complex and deeper analyzes are needed to confirm that this is the phenotype observed. Further analysis of the internal structures by electron transmission microscopy showed a higher number of vacuoles in the cytoplasm of TbVps15 RNAi cells. A similar phenotype was observed by downregulation of *T. brucei* PI4KIII [22], suggesting that phosphoinositides are important for the correct maintenance and organization of the internal cellular structures of this parasite. Additionally, it was possible to observe parasites that displayed an enlargement of the flagellar pocket, which is characteristic of cells where endocytosis is impaired [26]. Since this phenotype was not observed in all the analyzed population, we propose that TbVps15 is involved in bulk membrane endocytosis but it is not an essential component of this pathway.

As mentioned above, besides its role in autophagy, Vps34 plays a role in endocytosis and in intracellular transport in mammals and yeasts [2,27]. Furthermore, in the bloodstream form of *T. brucei* the PI3P showed a lysosomal localization and it was shown that the homologous protein TbVps34 is also involved in these processes [24]. Regarding TbVps15, the experiments with transferrin, dextran and Concanavalin A infer that its depletion reduces endocytosis rate, not being able to fully accumulate these markers in the lysosome.

Finally, protein kinase activity and PI3K activity were reduced in TbVps15 knockdown cells compared to uninduced parasites. The decrease in protein kinase activity may be because in addition to TbVp15 downregulation, its inhibition can affect some signaling cascade, thus affecting the activity of other protein kinases. On the other hand, there are no reports so far that show that Vps15 interacts with another PI3K in addition to Vps34, so we postulate that the decrease in PI3K activity observed corresponds to TbVps34, strengthening the concept that both proteins function together as part of a complex as it was demonstrated in *T. cruzi* [7]. However, we cannot rule out the possibility that the observed phenotypes may be the consequence of the inhibition of the TbVps15-TbVps34 complex by the downregulation of TbVps15. It is worth to highlight that this result points out the regulatory role of TbVps15 on TbVps34 enzymatic activity exposing a conservation of this pathway along eukaryotic cells.

T. brucei has a complex life cycle involving invertebrate and vertebrate hosts, and maintenance of the plasma membrane composition is essential for survival [28]. Part of this adaptation includes the specific stage differentiation of its endocytic system [26]. The fact that in *T. brucei* the protein TbVps15 is required for normal growth and endocytosis indicates that it is essential for *T. brucei* survival and postulate that this family of proteins may also be a potential target for anti-trypanosomal drugs.

Acknowledgments

We are very grateful to Dr. Tomas Falzone who generously provided us with red and green LysoTracker. This work was supported by the Consejo Nacional de Investigaciones Científicas y Técnicas (PIP 2013-00351); Departamento de Fisiología, Biología Molecular y Celular, Facultad de Ciencias Exactas y Naturales, Universidad de Buenos Aires (UBACyT 2014–2017, Nro 00155BA); and Agencia Nacional de Promoción Científica y Tecnológica (PICT 2013–2015 and PICT 2015-0898). G.D.A. and A.C.S. are members of the Research Career of Consejo Nacional de Investigaciones Científicas y Técnicas, T.S. is a fellow from the same institution and N.M.B. is fellow from the Agencia Nacional de Promoción Científica y Tecnológica. The funders had no

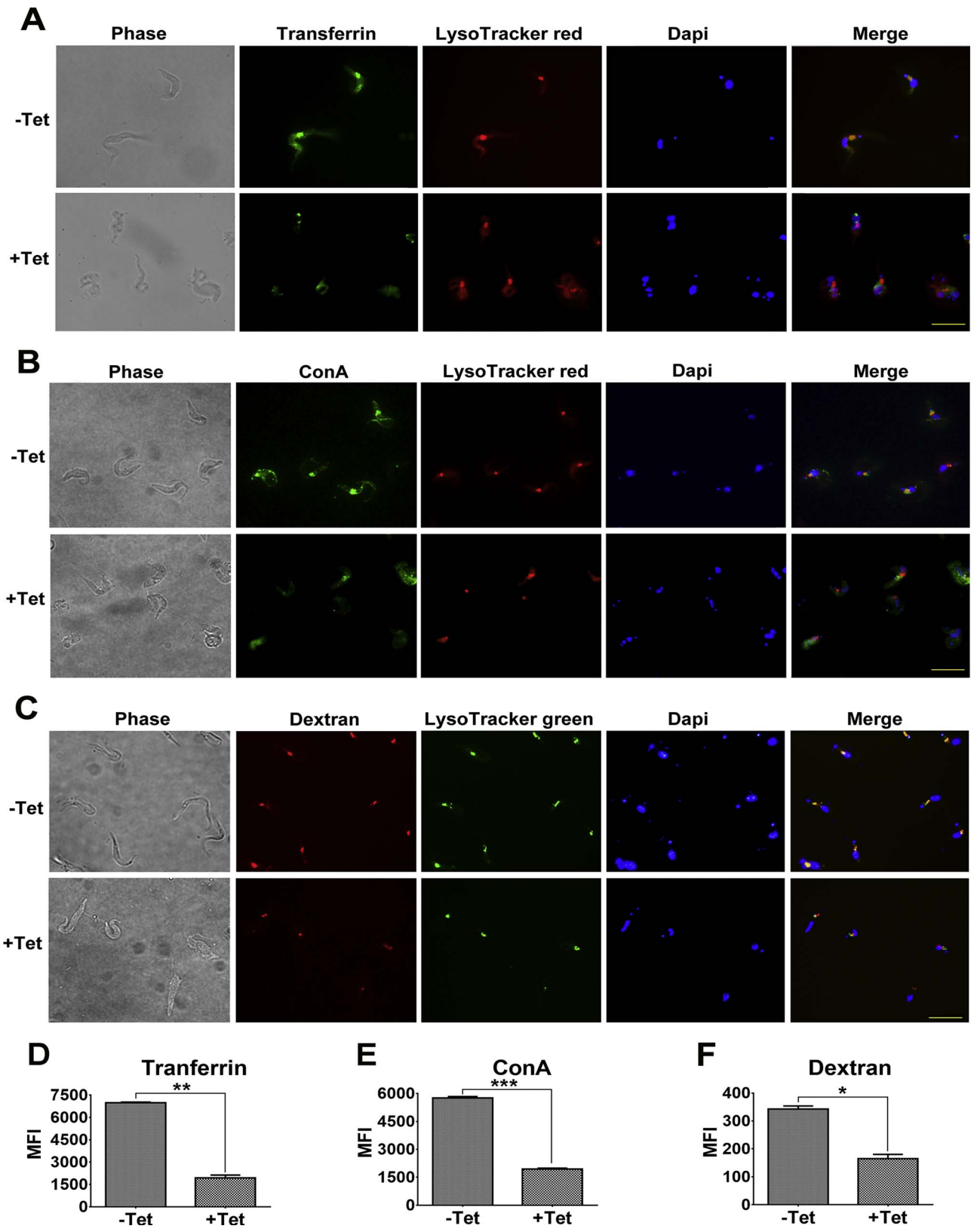

Fig. 5. TbVps15 RNAi shows diminished endocytosis and affected intracellular transport. TbVps15 RNAi cells were incubated in the absence (−Tet) or presence (+Tet) of tetracycline for three days and incubated with FITC-transferrin (**A**), FITC-ConA (**B**) and Alexa Fluor 546 dextran 10,000 MW (**C**) plus the lysosomal marker LysoTracker (red or green as appropriate), as described under "Materials and Methods". Treated cells were fixed, counterstained with DAPI to visualize the nucleus and kinetoplast and immediately visualized. Scale bars: 10 μm. **D**, **E** and **F** show quantification of uptake of transferrin, ConA and dextran respectively by flow cytometry. Mean values of fluorescence (in Arbitrary Units) and error bars representing the standard error of the mean (SEM) of three independent experiments are plotted. Asterisks denote significant differences ** p 0.011 for transferrin, *** p 0.004 for ConA and * p 0.148 for dextran, evaluated by Student's *t*-test. (For interpretation of the references to colour in this figure legend, the reader is referred to the web version of this article.)

role in study design, data collection and analysis, decision to publish, or preparation of the manuscript. The authors have no conflict of interest to declare.

Appendix A. Supplementary data

Supplementary data associated with this article can be found, in the online version, at http://dx.doi.org/10.1016/j.molbiopara.2017.11.004.

References

[1] J.M. Backer, The intricate regulation and complex functions of the Class III phosphoinositide 3-kinase Vps34, Biochem. J 473 (2016) 2251–2271, http://dx.doi.org/10.1042/BCJ20160170.

[2] C. Raiborg, K.O. Schink, H. Stenmark, Class III phosphatidylinositol 3-kinase and its catalytic product PtdIns3P in regulation of endocytic membrane traffic, FEBS J. 280 (2013) 2730–2742, http://dx.doi.org/10.1111/febs.12116.

[3] S.B. Thoresen, N.M. Pedersen, K. Liestol, H. Stenmark, A phosphatidylinositol 3-kinase class III sub-complex containing VPS15, VPS34, Beclin 1, UVRAG and BIF-1 regulates cytokinesis and degradative endocytic traffic, Exp. Cell Res. 316 (2010) 3368–3378, http://dx.doi.org/10.1016/j.yexcr.2010.07.008.

[4] Y. Araki, W.C. Ku, M. Akioka, A.I. May, Y. Hayashi, F. Arisaka, Y. Ishihama, Y. Ohsumi, Atg38 is required for autophagy-specific phosphatidylinositol 3-kinase complex integrity, J. Cell Biol. 203 (2013) 299–313, http://dx.doi.org/10.1083/jcb.201304123.

[5] S.F. Funderburk, Q.J. Wang, Z. Yue, The Beclin 1-VPS34 complex-at the crossroads of autophagy and beyond, Trends Cell Biol. 20 (2010) 355–362, http://dx.doi.org/10.1016/j.tcb.2010.03.002.

[6] A.C. Schoijet, K. Miranda, W. Girard-Dias, W. de Souza, M.M. Flawia, H.N. Torres, R. Docampo, G.D. Alonso, A *Trypanosoma cruzi* phosphatidylinositol 3-kinase (TcVps34) is involved in osmoregulation and receptor-mediated endocytosis, J. Biol. Chem. 283 (2008) 31541–31550, http://dx.doi.org/10.1074/jbc.M801367200.

[7] A.C. Schoijet, T. Sternlieb, G.D. Alonso, The phosphatidylinositol 3-kinase class III complex containing TcVps15 and TcVps34 participates in autophagy in *Trypanosoma cruzi*, J. Eukaryot. Microbiol. 64 (May (3)) (2017) 308–321, http://dx.doi.org/10.1111/jeu.12367 Epub 2016 Sep 23.

[8] A.C. Schoijet, K. Miranda, L.C.S. Medeiros, W. de Souza, M.M. Flawiá, H.N. Torres, O.P. Pignataro, R. Docampo, G.D. Alonso, Defining the role of a FYVE domain in the localization and activity of a cAMP phosphodiesterase implicated in osmoregulation in *Trypanosoma cruzi*, Mol. Microbiol. 79 (2011) 50–62, http://dx.doi.org/10.1111/j.1365-2958.2010.07429.x.

[9] G.D. Alonso, A.C. Schoijet, H.N. Torres, M.M. Flawiá, TcPDE4, a novel membrane-associated cAMP-specific phosphodiesterase from *Trypanosoma cruzi*, Mol. Biochem. Parasitol. 145 (2006) 40–49, http://dx.doi.org/10.1016/j.molbiopara.2005.09.005.

[10] B.S. Hall, C. Gabernet-Castello, A. Voak, D. Goulding, S.K. Natesan, M.C. Field, TbVps34, the Trypanosome orthologue of Vps34, is required for Golgi complex segregation, J. Biol. Chem. 281 (2006) 27600–27612, http://dx.doi.org/10.1074/jbc.M602183200.

[11] A. Balla, T. Balla, Phosphatidylinositol 4-kinases: old enzymes with emerging functions, Trends Cell Biol. 16 (2006) 351–361, http://dx.doi.org/10.1016/j.tcb.2006.05.003.

[12] E. Wirtz, S. Leal, C. Ochatt, G.A. Cross, A tightly regulated inducible expression system for conditional gene knock-outs and dominant-negative genetics in *Trypanosoma brucei*, Mol. Biochem. Parasitol. 99 (1999) 89–101.

[13] S. Redmond, J. Vadivelu, M.C. Field, RNAit: an automated web-based tool for the selection of RNAi targets in *Trypanosoma brucei*, Mol. Biochem. Parasitol. 128 (2003) 115–118.

[14] B. Wickstead, K. Ersfeld, K. Gull, Targeting of a tetracycline-inducible expression system to the transcriptionally silent minichromosomes of *Trypanosoma brucei*, Mol. Biochem. Parasitol. 125 (2002) 211–216.

[15] G.D. Alonso, A.C. Schoijet, H.N. Torres, M.M. Flawiá, TcrPDEA1, a cAMP-specific phosphodiesterase with atypical pharmacological properties from *Trypanosoma cruzi*, Mol. Biochem. Parasitol. 152 (2007) 72–79, http://dx.doi.org/10.1016/j.molbiopara.2006.12.002.

[16] A.R. Chowdhury, Z. Zhao, P.T. Englund, Effect of hydroxyurea on procyclic *Trypanosoma brucei*: an unconventional mechanism for achieving synchronous growth, Eukaryot. Cell 7 (2008) 425–428, http://dx.doi.org/10.1128/EC.00369-07.

[17] R. Kieft, P. Capewell, C.M.R. Turner, N.J. Veitch, A. MacLeod, S. Hajduk, Mechanism of *Trypanosoma brucei gambiense* (group 1) resistance to human trypanosome lytic factor, Proc. Natl. Acad. Sci. U. S. A. 107 (2010) 16137–16141, http://dx.doi.org/10.1073/pnas.1007074107.

[18] K. Miranda, M. Benchimol, R. Docampo, W. de Souza, The fine structure of acidocalcisomes in *Trypanosoma cruzi*, Parasitol. Res. 86 (2000) 373–384 http://www.ncbi.nlm.nih.gov/pubmed/10836511 (Accessed 8 November 2017).

[19] L.C. Soares Medeiros, F. Gomes, L.R.M. Maciel, S.H. Seabra, R. Docampo, S. Moreno, H. Plattner, J. Hentschel, U. Kawazoe, H. Barrabin, W. de Souza, R.A. Damatta, K. Miranda, Volutin granules of eimeria parasites are acidic compartments and have physiological and structural characteristics similar to acidocalcisomes, J. Eukaryot. Microbiol. 58 (2011) 416–423, http://dx.doi.org/10.1111/j.1550-7408.2011.00565.x.

[20] C. Panaretou, J. Domin, S. Cockcroft, M.D. Waterfield, Characterization of p150, an adaptor protein for the human phosphatidylinositol (PtdIns) 3-kinase. Substrate presentation by phosphatidylinositol transfer protein to the p150. Ptdins 3-kinase complex, J. Biol. Chem. 272 (1997) 2477–2485 http://www.ncbi.nlm.nih.gov/pubmed/8999962 (Accessed 27 April 2017).

[21] P.K. Herman, J.H. Stack, J.A. DeModena, S.D. Emr, A novel protein kinase homolog essential for protein sorting to the yeast lysosome-like vacuole, Cell 64 (1991) 425–437.

[22] M.J. Rodgers, J.P. Albanesi, M.A. Phillips, Phosphatidylinositol 4-kinase III-beta is required for Golgi maintenance and cytokinesis in *Trypanosoma brucei*, Eukaryot. Cell 6 (2007) 1108–1118, http://dx.doi.org/10.1128/EC.00107-07.

[23] S. Christoforidis, M. Miaczynska, K. Ashman, M. Wilm, L. Zhao, S.C. Yip, M.D. Waterfield, J.M. Backer, M. Zerial, Phosphatidylinositol-3-OH kinases are Rab5 effectors, Nat. Cell Biol. 1 (1999) 249–252, http://dx.doi.org/10.1038/12075.

[24] B.S. Hall, C. Gabernet-Castello, A. Voak, D. Goulding, S.K. Natesan, M.C. Field, TbVps34, the trypanosome orthologue of vps34, is required for golgi complex segregation, J. Biol. Chem. 281 (2006) 27600–27612, http://dx.doi.org/10.1074/jbc.M602183200.

[25] E.F. Hendriks, D.R. Robinson, M. Hinkins, K.R. Matthews, A novel CCCH protein which modulates differentiation of *Trypanosoma brucei* to its procyclic form, EMBO J. 20 (2001) 6700–6711, http://dx.doi.org/10.1093/emboj/20.23.6700.

[26] C.L. Allen, D. Goulding, M.C. Field, Clathrin-mediated endocytosis is essential in *Trypanosoma brucei*, EMBO J. 22 (2003) 4991–5002, http://dx.doi.org/10.1093/emboj/cdg481.

[27] P.K. Herman, S.D. Emr, Characterization of VPS34, a gene required for vacuolar protein sorting and vacuole segregation in *Saccharomyces cerevisiae*, Mol. Cell. Biol. 10 (1990) 6742–6754.

[28] S.K. Natesan, L. Peacock, K. Matthews, W. Gibson, M.C. Field, Activation of endocytosis as an adaptation to the mammalian host by trypanosomes, Eukaryot. Cell 6 (2007) 2029–2037, http://dx.doi.org/10.1128/EC.00213-07.